Reconciling longwall gob gas reservoirs and venthole production performances using multiple rate drawdown well test analysis

C. Özgen Karacan *

National Institute for Occupational Safety and Health (NIOSH), Pittsburgh Research Laboratory, Pittsburgh 15236, PA, USA

A B S T R A C T

Longwall mining is an underground mining method during which a mechanical shearer progressively mines a large block of coal, called a panel, in an extensive area. During this operation the roof of the coal seam is supported only temporarily with hydraulic supports that protect the workers and the equipment on the coal face. As the coal is extracted, the supports automatically advance and the roof strata cave behind the supports. Caving results in fracturing and relaxation of the overlying strata, which is called "gob." Due its highly fractured nature, gob contains many flow paths for gas migration. Thus, if the overlying strata contain gassy sandstones or sandstone channels, gas shales or thinner coal seams which are not suitable for mining, then the mining-induced changes can cause unexpected or uncontrolled gas migration into the underground workplace. Vertical gob gas ventholes (GGV) are drilled into each longwall panel to capture the methane within the overlying fractured strata before it enters the work environment. Thus, it is important, first to understand the properties of the gas reservoir created by mining disturbances and, second, to optimize the well parameters and placement accordingly.

In this paper, the production rate-pressure behaviors of six GGVs drilled over three adjacent panels were analyzed by using conventional multi-rate drawdown analysis techniques. The analyses were performed for infinite acting and pseudo-steady state flow models, which may be applicable during panel mining (DM) and after mining (AM) production periods of GGVs. These phases were analyzed separately since the reservoir properties, due to dynamic subsidence, boundary conditions and gas capacity of the gob reservoir may change between these two stages. The results suggest that conventional well test analysis techniques can be applicable to highly complex gob reservoirs and GGVs to determine parameters such as skin, permeability, radius of investigation, flow efficiency and damage ratio. The insights obtained from well test analyses can be used for a better understanding of the gob and for designing more effective gob gas venthole systems.

1. Introduction—establishing the need for well test analyses of the "gob"

1.1. Generation and properties of "gob" reservoir during longwall mining

Longwall mining occurs in a large, rectangular area, called a "panel," outlined by ventilation entries. During mining of a panel, roof rocks are temporarily supported with hydraulic supports to protect the workers and the equipment. As the coal is extracted from the panel, the supports automatically advance and the roof strata are allowed to cave behind. The caved zone created during this process is highly fragmented, and generally extends upwards three to six times the thickness of the mined coal bed. Caving results in relaxation of the overlying strata that is characterized by mining-induced vertical and horizontal fractures and bedding plane separations (Fig. 1). The caved and overlying fractured zone collectively is called the "gob".

Fracturing and relaxation in the gob creates new and highly permeable flow paths. Methane inflow from the gob into the mining environment is influenced by the magnitude of fracturing and the extent to which the fractures stay open during mining. Singh and Kendorski (1981) evaluated the disturbance of rock strata resulting from mining and described a caved zone that extends from the mining level to 3 to 6 times the seam thickness, a fractured zone that extends from the mining level to 30 to 58 times the seam thickness, a bending zone where there is no change in permeability that extends from 30 times the seam thickness to 50 ft below ground surface. Any gas that is contained within the gob will be released over time and is a big contributor to emissions, if not controlled (Fig. 1). Relaxation of the roof rocks and the associated fracture connectivity allows gas to flow from all surrounding gas sources toward the mine workings, which eventually may create an unsafe condition for the underground workforce. Also, depending on how the venthole interacts with the gob and mining environment, there may be some ventilation air

* Tel.: +1 412 386 4008; fax: +1 412 386 6595.
E-mail address: cok6@cdc.gov.

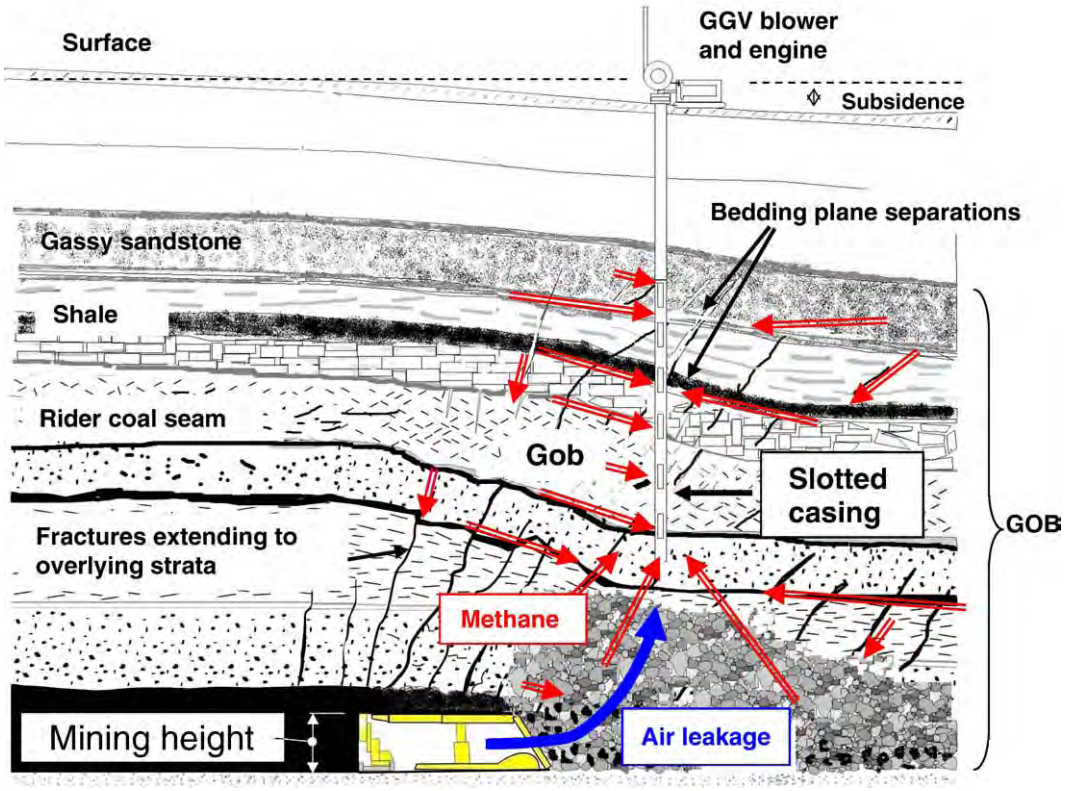

Fig. 1. A schematic representation of longwall mining with a shearer. The figure shows the fractures extending the overlying strata, bedding plane separation, subsidence and possible methane flow paths (red arrows) and air leakage from the face (blue arrow). A schematic of a GGV producing this gas is also shown.

leaking from the face into the gob and produced along with the captured methane (Fig. 1).

The characteristics of fracturing and the subsidence of overburden are revealed through predictive techniques and field studies (Luo, 1989; Cui et al., 2001; Palchik, 2005; Li et al., 2005). It was concluded that rock failure leading to increased hydraulic conductivity in the gob was initiated by high compressive stresses ahead of the face with the fractures subsequently opened by tensile stresses behind the face (Liu and Elsworth, 1997). Gale (2005) reported that the horizontal conductivity can be significantly enhanced along bedding planes within and well outside the panel. This probably will vary depending on the nature of each site as reported by Whittles et al. (2006, 2007).

As mining progresses, the caved zone in the gob gradually consolidates sufficiently to support large loads resulting from the overburden weight (Pappas and Mark, 1993). Consolidation results in a reduction in the porosity and the associated permeability. Although reduced to some degree due to compaction, prevailing high permeability pathways in the gob still affect the flow of methane from surrounding sources into the gob and into the mine. Thus, an understanding of resultant reservoir properties of gob material is very important for developing adequate methane control strategies.

1.2. Gob gas ventholes "GGV" and their use in methane production and control

One common technique to control methane emissions is to drill vertical gob gas ventholes (GGV) into each longwall panel to capture the methane within the overlying fractured strata before it enters the work environment. Gob gas ventholes are commonly used to control the methane emissions from the fractured zone and are drilled from the surface to a depth that places them above the caved zone. The bottom section of the pipe is slotted and placed adjacent to the expected gas production zone (Fig. 1).

Although the drilling practices of GGVs may change based on local conditions, most gob gas ventholes are drilled to within a short distance, 35–100 ft, of the coal bed and cased with steel pipe. Commonly, the bottom section of the casing, generally about 200 ft, is slotted (Fig. 2-A and B). The casing is cemented using 2–3 cement baskets (Fig. 2-C) above the slotted section. Thus, the slotted section remains open to the gob and supported by the cemented casing string from the surface. The usual practice is to drill the gob gas ventholes prior to mining. As mining advances under the venthole, the gas-bearing strata that surround the wellbore will fracture and will establish preferential pathways for the released gas, or the leaking mine air, to flow towards the ventholes (Diamond, 1994) as shown in Fig. 1.

Exhausters are placed on gob gas ventholes (Fig. 1) to maintain a vacuum on the wellbore to induce gas flow towards the venthole. Gas production may exhibit variable gas quality. In the early stages of production, the gas quality is generally high (>80%) after a hole is intercepted by the longwall. Relatively high production rates with high methane quality are usually sustained for a few weeks. Later in time, especially towards the end of the panel mining or after the panel is completed, gob gas production may exhibit decreased methane levels as ventilation air is drawn from the active mine workings. The quality of the gas from GGVs can be controlled to some extent by varying the vacuum on the wellhead to correspond with the profile of expected methane release. However, for mine safety, maintaining the methane concentration in the mine within statutory limits is always the overriding factor for controlling the vacuum on the gob gas ventholes, as it is for all other mine-related methane drainage systems. Thus, commonly, when the methane concentration in the produced gas reaches 25%, the exhausters are de-energized as a safety measure and the holes may be allowed to free flow. Therefore, from a production point of view, there are two primary phases in the producing life of a GGV: 1—production during panel mining (DM) and 2—production period after panel is mined out (AM).

Fig. 2. A pictorial showing of a slotted casing ready to be lowered (A), the dimension of each of the slots (B) and the baskets (C) used above the slotted interval to stop the cement to flow beyond intended interval.

It is difficult to predict production performance of gob gas ventholes due to the involvement of multiple influential factors, complex properties of the gob, and due to the lack of knowledge on interactions of the GGV with the gob reservoir. Currently, a standard approach that can realistically represent the multiple variables associated with underground coal mining operations and their interactions and influences on the performance of gob gas ventholes does not exist. This may be related to the non-existence of enough field tests and the actual reservoir data obtained using these tests and the challenges and unknowns related to the gob environment. There have been some modeling studies for predicting GGV performance (Lunarzewski, 1998; Ren and Edwards, 2002; Palchik, 2002; Tomita et al., 2003; Karacan et al., 2005, 2007). However all of these models rely on predicted permeabilities based on geomechanical calculations. Thus, despite the improvements detailed in these studies, experience suggests that it is still difficult to accurately predict methane production from a GGV. At this juncture, transient well tests analyses methods, such as multi-rate drawdown, and interference and pressure build-up tests that are applied in the petroleum and natural gas industry and in coalbed methane reservoirs (Matthews and Russell, 1967; Earlougher, 1977; Dake, 1978; Lee, 1982; King et al., 1986; Mohaghegh and Ertekin, 1991; Mavor and Saulsberry;, 1996; Engler and Tiab, 1996; Nashawi, 2008) can be reliable tools to understand the characteristics of the gob reservoir and the interaction of GGVs with the gob and mining environment.

1.3. Purpose of this study

Improvements in venthole gas drainage evaluation and prediction capabilities for site-specific mining conditions and circumstances can address longwall gas emission issues, resulting in ventholes designed for optimum production and mine safety and also for improved gas capture. Thus, the objective of this paper is to make an attempt using multi-rate drawdown gas well tests analyses to understand the behavior of the gob gas ventholes and the reservoir properties of the gob. In order to achieve this objective, the production rate-wellhead pressure behavior of six gob gas ventholes drilled over three different panels was analyzed using F.A.S.T WellTest® (Fekete Associates, 2009) for parameters such as skin, permeability, radius of investigation, flow efficiency and damage ratio for a better reservoir understanding of the gob and the GGVs. In these analyses, the GGV production periods during panel mining (DM) and after mining (AM) were analyzed separately, using multi-rate production drawdown analyses techniques using infinite flow and pseudo-steady state (PSS) flow models, respectively, since the reservoir capacity, behavior and gas production potential changed between these two phases.

2. Description of overburden stratigraphy in the study area and locations of GGVs

2.1. Overburden stratigraphy and the effects on formation of gob reservoir

This study has been conducted in the Northern Appalachian Basin in Southwestern Pennsylvania, in Greene County, Pennsylvania. This area is very important for coal mining and for mining-related methane emissions and capture using conventional boreholes and gob gas ventholes.

In the study area, most of the longwall mining operations exist in the Pittsburgh seam of the Monongahela Group and the methane emissions from the gobs of these operations are captured using GGVs. The Monongahela Group is located within the Pennsylvanian age sediments and includes the interval from the base of the Pittsburgh coal to the top of the Waynesburg coal. The general coal measures in the Monongahela Group in Greene County and their thicknesses from top to bottom of the group, can be listed as: shale (0 to 11.8 ft), Waynesburg main coal bed (5.9 ft), clay (2.95 ft), sandstone (19.7 ft), limestone (5 ft), sandstone and shale (60 ft), Uniontown coal bed (1 ft to 3 ft), Upper Great limestone (17.7 ft), sandstone and shale (60 ft), Lower Great limestone (55.1 ft), sandy shale (40 ft), Sewickley coal

bed (1 to 6 ft), sandstone (9.8 ft), the Fishpot limestone (17.7 ft), sandstone and shale (25 ft), Redstone coal bed (1 to 3.9 ft), limestone (9.8 ft), Pittsburgh upper sandstone (40–50 ft—sandstone paleochannel), shale (0 to 9 ft), and Pittsburgh coal bed (5 to 12.1 ft) (Penn State University Libraries, 2000). Markowski (1998) reported that the main coal beds that are consistent and continuous in the study area of this paper are the Pittsburgh, Sewickley, and Waynesburg. The Redstone coal bed and Pittsburgh rider coals are not continuous and can be present at some locations. In this interval, the Sewickley coal bed, the gassy sandstones within the gob interval and the Redstone and rider coals are believed to be the main source of gob methane produced by GGVs.

Fig. 3 shows three stratigraphic plots of these layers at three example core-hole locations and the relative location of the slotted casing in these boreholes. In order to show these thicknesses of different strata at the same depth level, a depth correction procedure was applied to the core-hole data (Karacan and Goodman, 2009). This procedure allowed the rock layers, their thicknesses and the slotted casing locations to be compared in the same depth scale (Fig. 3).

The example core logs given in Fig. 3 show that the thicknesses and the presence or absence of layers change based on their locations. For instance, in the first log, there is a thick sandstone layer (sandstone paleochannel) above the Pittsburgh coal bed, which is present but not dominant in the other two logs. And when it exists, depending on its thickness, the bottoms of the slotted casings of the ventholes are either in this sandstone or over it within a close proximity. Similarly, the last two logs have thick limestone layers about 140 ft above the Pittsburgh coal bed. Also, the number and thicknesses of other shale–sandstone sequences are different in each location. This is characteristic of coal measure strata deposited in swamp and lacustrine environments (Karacan, 2009). More importantly, the existence and thicknesses of these layers at various borehole locations impact the caving, fracturing and bedding plane separations in the overburden during longwall mining. This eventually affects the formation of the gob reservoir, gas availability and production of GGVs.

In the gob, horizontal fractures occur along weak-strong rock layer interfaces during the movement of the overburden. The formation, thickness and location of horizontal fractures influence the hydraulic conductivity of the overburden strata, which creates methane emission pathways and controls methane emissions into the mine. The fractures are usually correlated with uniaxial compressive strength and thickness of rock layers, distances from the extracted coal seam to the rock layer interfaces, and the thicknesses of extracted coal seams (Palchik, 2002).

In the study area, based on an investigation of hydraulic conductivities and the estimation of strata fracturing (Karacan and Goodman, 2009), it is more probable that fracturing and bedding plane separations will occur within an interval between 40 ft and

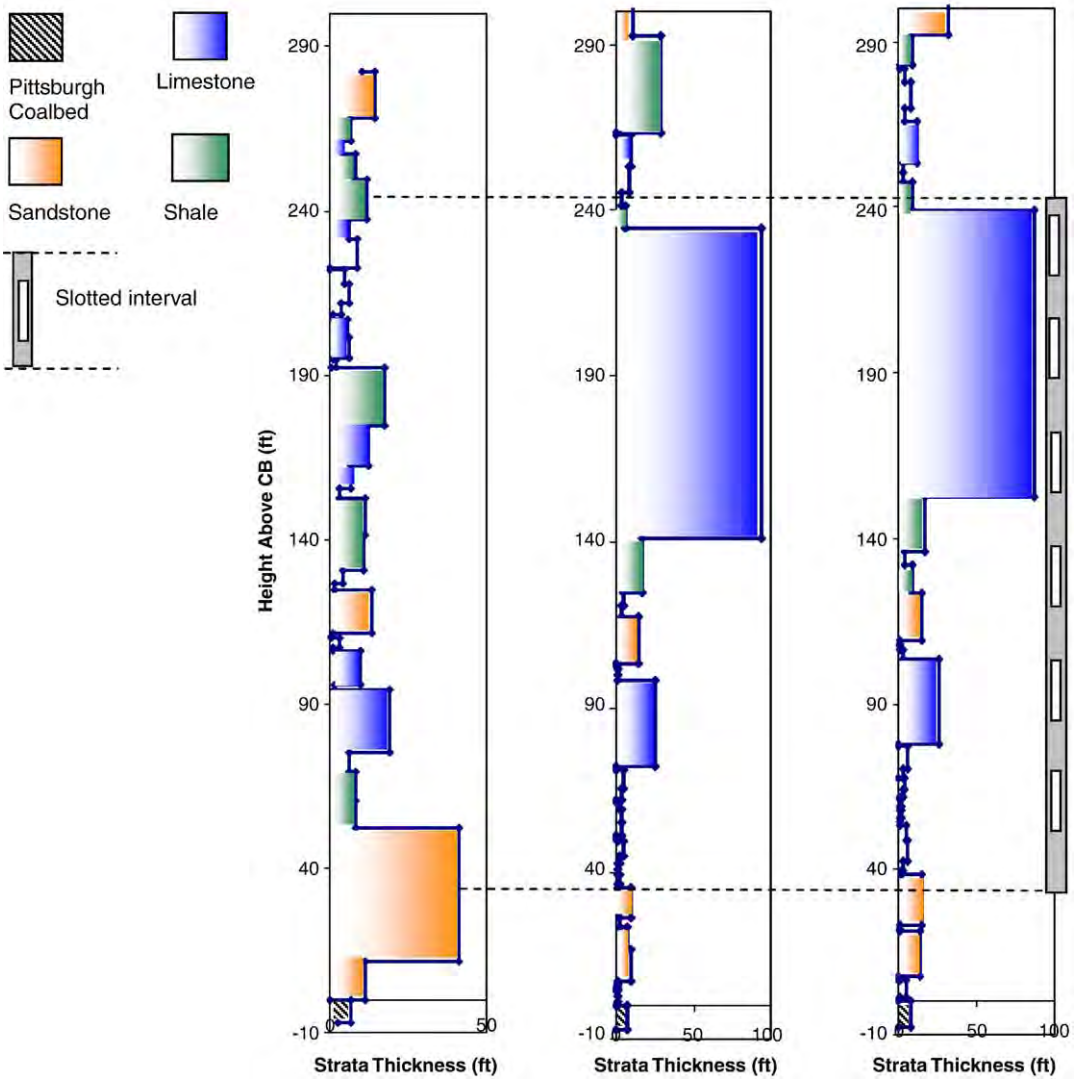

Fig. 3. Stratigraphic log and thicknesses of the formations at three example core-hole locations in the study area.

145 ft from the top of coal bed. This interval contains thin limestones, sandstones and weaker strata, such as coalbeds and shales (Karacan and Goodman, 2009).

2.2. Location effects on the gob gas venthole production performances

The production performance of gob gas ventholes are closely related to their locations on the panels, borehole completions, wellhead designs, and the operation of the exhausters (Diamond, 1994; Ren and Edwards, 2002; Karacan et al., 2007; Karacan and Goodman, 2009; Karacan, 2009). These may be important in interpretation of the well test behaviors and results as well. Thus, a few of the possible factors on gob gas venthole production-pressure behavior will be summarized in this section.

Table 1 gives the actual drilling and location details of the 6 ventholes monitored for their production performance in this study. As this table shows, panel dimensions, location details and venthole completion details differ. Thus, varying production performances can be expected from these ventholes.

These boreholes were drilled on three adjacent panels (1B to 3B) as indicated in the first column of Table 1. The second numbers are the GGV number on each panel. Each borehole was completed with 200-ft of slotted casings, shown in Fig. 2. Due to the terrain of the study site and the land ownership issues, each borehole was located at varying elevations above sea level. Thus, the boreholes with highest elevations are 1B-1, 2B-2 and 2B-3. Accordingly, the drill depths to the top the slotted casing and the overburden depths are highest in these boreholes. However, 2B-2 is closest to the tailgate entries of 2B panel, which possibly locates this borehole in the tension zone around the edges of the panel, where fractures are more open. Close-to-margin placements of the ventholes and its possible effect on production difference of the ventholes, as the reservoir properties change in cross-panel direction during transition from tension to compression, are also one of the underlying assumptions of using a composite model as the reservoir geometry in the well test analyses as will be discussed in the next sections.

The GGVs do not have separate production tubing installed and production is achieved through the casing. Table 1 shows that the casing diameters used in monitored boreholes are 7 and 8 in. Keeping the other completion parameters constant, increasing the gob gas venthole diameter increases cumulative methane production from the subsided strata (Karacan et al., 2007). Although a marginal decrease in the methane concentration can be seen from this change, possibly due to increased mine air extraction with a larger sink, the increased gas flow rate increases the overall volume of methane produced.

Distance of the slotted casing to the coal bed may also play an important role on the amount and concentration of methane captured. Reservoir modeling results (Karacan et al., 2007) showed that when the setting depth was close to or within the caved zone, the methane concentration and the total amount of methane captured decreased. However, one additional consideration for changing the setting depth for the slotted casing may be the competency and productivity of the formations surrounding the slotted casing based on their mechanical properties and gas contents.

The distances from the start of the panels and the distances between the ventholes along the panel are again based on maximizing productivity, on the expected drainage radius of the ventholes, and on the emissions into the mines. It has been shown that the location of the ventholes on the panel is important for their performance (Diamond, 1994). In general, the first holes on the start end of the panels are the highest-quantity and longest-duration producers. This is attributed to enhanced mining-induced fractures where the overburden strata are in tension and open to flow with higher permeabilities. Table 1 shows that three boreholes in this study (1B-1, 2B-1 and 3B-1) are the first boreholes in respective panels. However, 1B-1 was surrounded by virgin coal seam since it was the first borehole in this new district and 3B-1 was located in a wider panel compared to 1B and 2B. Thus, these differences may have implications on the flow-pressure data and on well test results.

Fig. 4 shows the locations of the ventholes monitored in this study on a 3-D surface elevation and on the sandstone paleochannel thickness maps. The bottom diagram in this figure is an overlay of the mine map showing the panels with the sandstone channel thickness contours with a projection of borehole locations.

Fig. 4 shows that ventholes are located on rough terrain, which is characteristic to the Appalachian basin. Some of the ventholes are located on hill sides or tops and others close to the valley bottoms. However, besides this and the other issues discussed on the possible effects of borehole location on production performance, it should be noted that 2B-2 and 3B-1 are located in a region (Fig. 4, bottom diagram) where there is either no sandstone channel or it is too thin to have a major effect on caving and gob formation. On the other hand 1B-1 and 2B-1 are in a region where sandstone channel thickness is between 0 and 20 ft, and 2B-3 is in a location where sandstone thickness is between 20 and 40 ft. 2B-4 is located in the thickest section of the sandstone (>40 ft), where the slotted casing is either in the sandstone or very close to the top of the paleochannel. The presence and absence of this channel and its thickness is expected to be very influential on the caving behind the shields and below the ventholes. In situations where the roof material is stiff and thick, it cantilevers behind the shields leading to a lesser degree of fracturing in overlying strata and impeding development of high permeability fractures around the borehole. Since the rock strength of sandstone is much more than the shale-type formations, different subsidence and thus venthole production histories can be expected based on this factor.

3. Monitoring of the ventholes for production and pressures

3.1. Instrumentation of the gob gas ventholes

The six gob gas ventholes (Table 1; Fig. 4) that were drilled, completed and monitored in this study were instrumented prior to undermining their locations. As it was discussed in the introduction section, these boreholes generally do not produce any fluid before the

Table 1
Drilling, location and borehole details of the 6 ventholes monitored for their production history in this study.

GGV	Surface elevation (ft)	Distance to tailgate entry (ft)	Depth to bottom of slotted pipe (ft)	Over burden (ft)	Venthole diameter (in.)	Dist. to coal bed (ft)	Dist. from panel start (ft)	Panel length (ft)	Panel width (ft)
1B-1	−1356.80	232	793.80	828.80	7	35	550	11,030	1225
2B-1	−1166.16	305	599.16	644.16	8	45	372	10,798	1225
2B-2	−1321.76	223	744.76	789.76	8	45	2132	10,798	1225
2B-3	−1383.81	274	799.81	844.81	7	45	4492	10,798	1225
2B-4	−1294.00	238	691.00	731.00	7	40	6872	10,798	1225
3B-1	−1143.00	283	585.00	630.00	7	45	482	11,086	1425

In elevation data, sea level is zero and higher elevations are in negative direction.

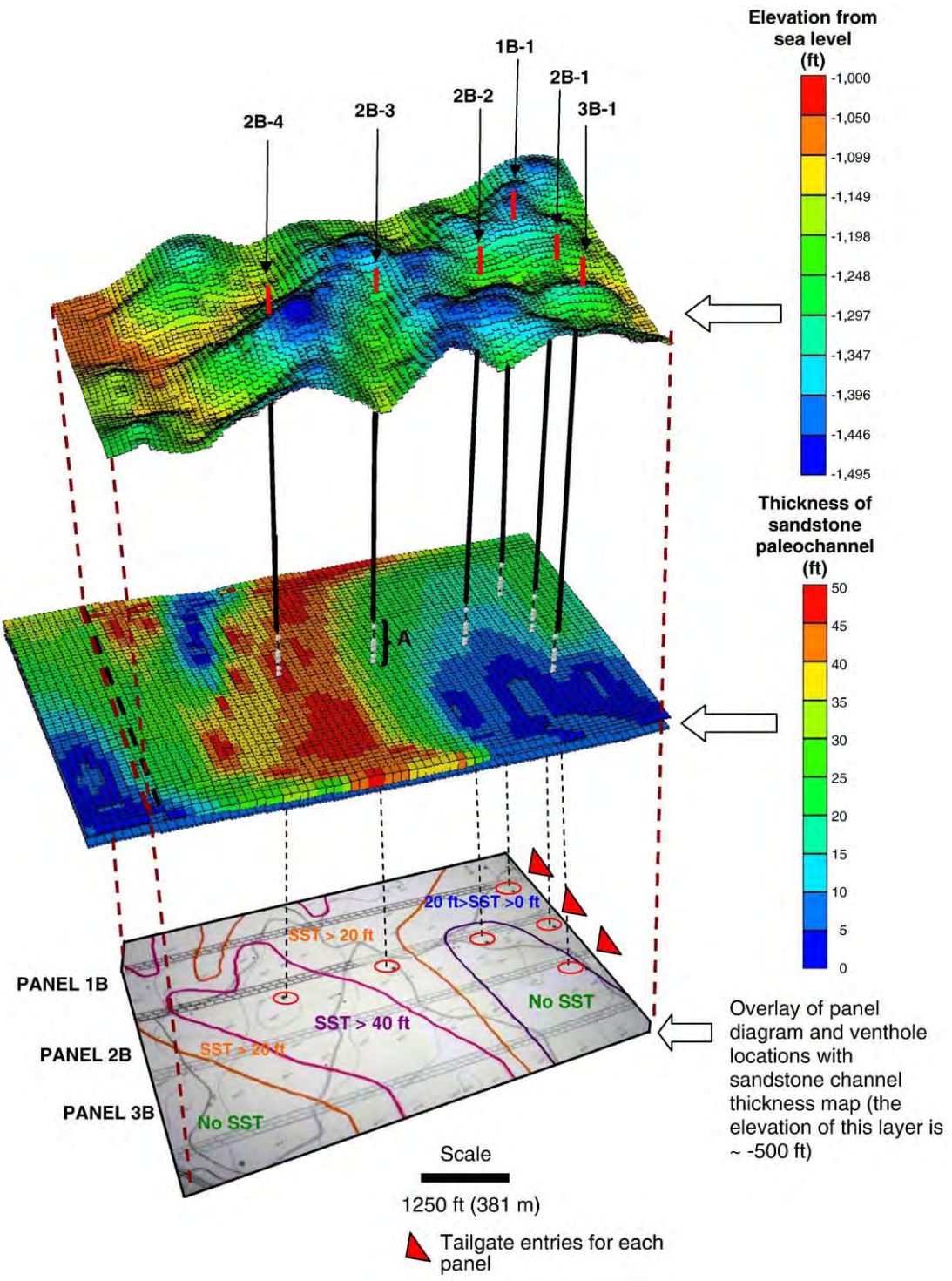

Fig. 4. A composite figure showing the surface elevation, sandstone thickness above the mined coal seam and mine map. This figure shows the approximate location of the ventholes on the surface, the longwall panels and the relative positions of the panels and the ventholes with respect to the various thicknesses of the sandstone channel. "A" in the middle figure is the section where the ventholes have slotted casings.

strata is fractured as a result of undermining. After fracturing, these boreholes produce gas of varying methane concentration throughout the mining of the panel, even after panel completion, until the methane concentration decreases to low levels. Thus, the total gas production phase of a gob gas venthole can be described as the production during panel mining (DM) and after completion of the panel (AM). Water, which accumulates in the borehole in some cases, flows into the gob during undermining and is not produced at the surface. The total gas production in these ventholes comes from different sources at different depths of the slotted casing interval and was produced as a mixed gas stream by a methane-driven exhauster that provided vacuum at the wellhead.

Ideally, for transient behavior of production and pressure, the boreholes should be instrumented downhole to measure the flowing bottom-hole pressure and the rates. Since these boreholes are closely related to the underground safety of the miners, maintaining intrinsic electrical safety is a must with any instrumentation used in the downhole to prevent possibility of an accident. To avoid these risks,

the boreholes were instrumented on the surface before the exhauster with flow meters, methanometers, thermocouples and pressure transducers to measure the total flow rate, methane percentage, temperature and pressure at the wellhead. Considering the fact that the boreholes were not very deep and there was no standing water column in the boreholes, measuring and using wellhead values, as opposed to downhole measurements, in well test calculations can be considered a reasonable approach.

3.2. Venthole production and pressure data

Fig. 5 (A–D) shows the total gas production (A–B) and wellhead pressure (C–D) history of monitored gob gas ventholes during mining (A–C) and after completion of panels (B–D). The production times in these figures are the elapsed times since the boreholes first started to produce gas during mining and the production times after the completion of the respective panels. Although the data is scattered, the general trends in observed gas productions show that the ventholes initially produced at higher gas rates and then the rates either stabilized or entered a decline period with increasing time. Four of the six boreholes (1B-1, 2B-1, 2B-2 and 2B-3) continued producing after the panel, over which they were located, was completed. However, this production phase had a faster decline compare to the during-mining phase.

Comparison of Fig. 5-A and B with Fig. 5-C and D, respectively, shows that total gas production rate was generally correlated with applied vacuum (wellhead pressure). Although a vacuum applied to the gob gas ventholes stimulates methane migration into the ventholes from the surrounding strata and prevents occasional flow reversals (Thakur, 2006), this advantage may be lost over time as there is tendency for mine air to be drawn into the gob area and to dilute the methane (Ren and Edwards, 2002). A higher suction pressure has a positive but relatively small effect on drawing gas from overlying strata into the venthole. In the monitored ventholes, the wellhead pressures were generally between 11.5 and 13.0 psia (Fig. 5-C and D) and the wellhead pressures were generally lower during the panel mining phase of gas production compared to production after the panels were completed. This may due to a lower methane flow rate.

Fig. 6 shows the methane concentration in the total gas production of monitored gob gas ventholes during mining (6-A) and after completion of panels (6-B) as well as methane flow rates measured at the wellhead for these two flow phases (C and D). The data show that during mining, 1B-1 and 3B-1 had the highest methane percentage (80–90%) in production. Both of these wells were the first ventholes in the respective panels. The ventholes of 2B panel produced with ~50% methane. The rest of the produced gas was air sucked from the mining environment through gob (Fig. 1). The methane flow rate (6-C), on the other hand, was highest in 2B-2 venthole and lowest in 2B-4 during panel mining, which may be related to location of the ventholes.

After the panels were completed, methane percentages decreased somewhat (6-B) compared to the DM phase (6-A). However, a marginal methane percentage increase was observed in 2B-1 and 2B-2. Between DM and AM phases, methane flow rates decreased from an average rate of 0.25 MMscf/day (6-C) for all the ventholes, except 2B-2, to 0.1 MMscf/day (6-D). The methane flow rate of 2B-2 stayed almost stable around 0.3 MMscf/day, making this venthole stand out among others.

Table 2 gives the mean, standard deviation, minimum and maximum values of total gas production rate and wellhead pressure data presented in Fig. 5, along with production durations of each venthole during and after panel mining.

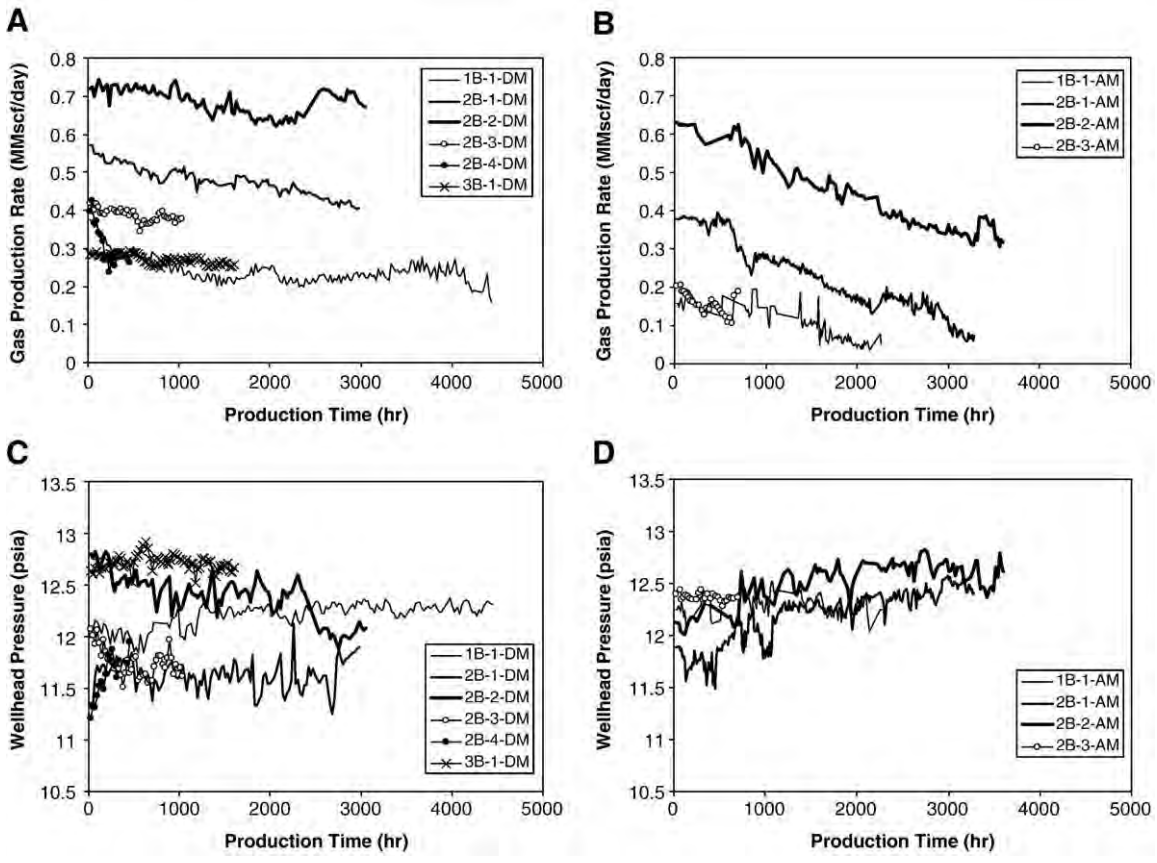

Fig. 5. Total gas production (A–B) and wellhead pressure (C–D) history of monitored gob gas ventholes during mining (A–C) and after completion of panels (B–D).

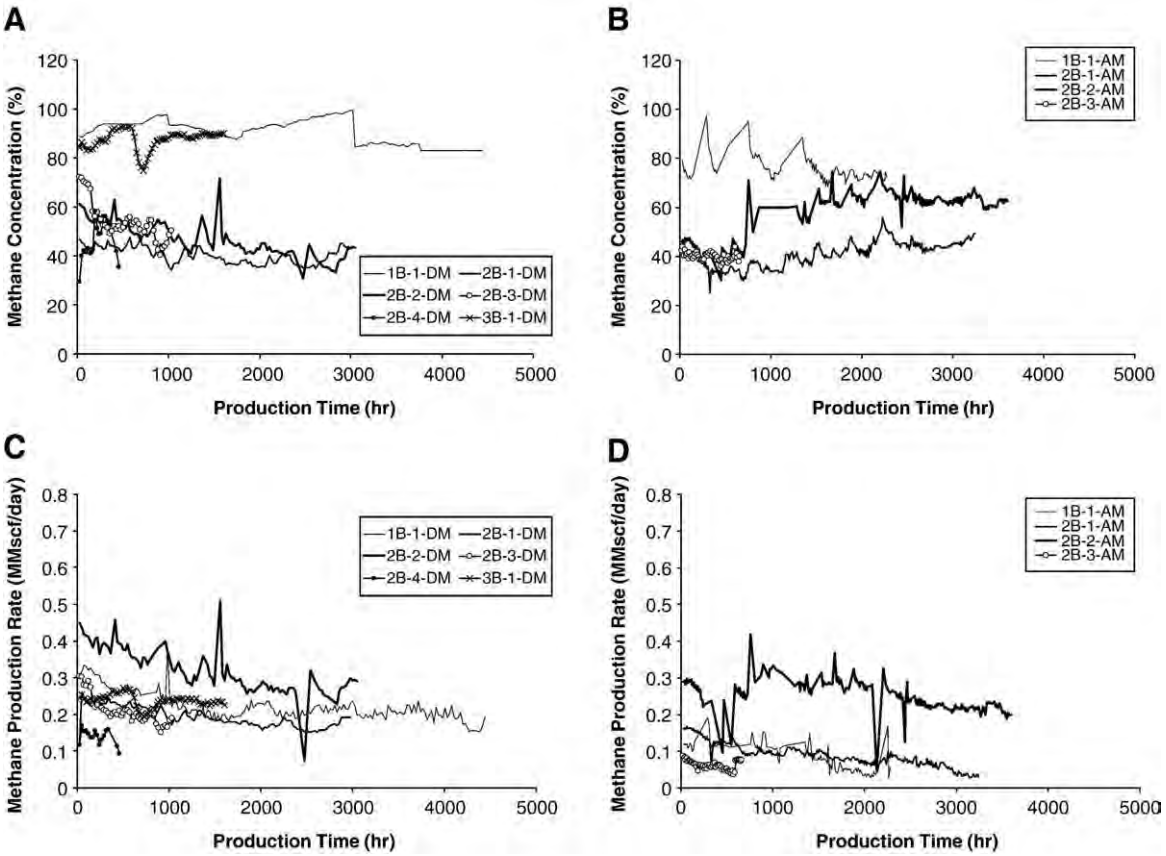

Fig. 6. Methane percentage (A–B) and measured methane flow rate (C–D) from monitored gob gas ventholes during mining (A–C) and after completion of panels (B–D).

4. Application of multi-rate well testing method for gob gas ventholes

In this study, the gas flow rates (total and methane) and the flowing pressures at the wellheads of six ventholes were measured as a function of time during panel mining and after panel completion (Figs. 5 and 6). In order to evaluate these data and to gain insights about the ventholes' production behaviors and the reservoir properties of gobs, an analysis was carried out by using conventional multi-rate drawdown gas well testing methods. In the well test analysis study, F.A.S.T. WellTest (Fekete Associates, 2009) software was used to evaluate total gas production and wellhead pressure data. The data matching and linear regression plots to semi-log and log–log data were performed using the built-in APE (Automated Parameter Estimation) algorithm. Single-well, radial-composite models were used for infinite acting and pseudo-steady state flow periods during panel mining (DM) and after panel completion (AM) production phases of the ventholes, respectively.

4.1. Basic assumptions and their justifications for analyzing GGVs using conventional well testing methods

Some assumptions were made during analysis of the flow rate-pressure data. First of all, it was assumed the flow is radial towards the venthole within the slotted length of the gob. Normally, the flow regime in gob reservoirs is highly complex due to its nature (Fig. 1). There may be linear flow components around the boreholes due to the existence of fractures. However, radial flow was assumed within the whole reservoir in the absence of fracture width and length information. It is difficult to measure these properties since they

Table 2
Mean, standard deviation, minimum and maximum values of production rate and wellhead pressure data presented in Fig. 5.

	1B-1-DM	2B-1-DM	2B-2-DM	2B-3-DM	2B-4-DM	3B-1-DM	1B-1-AM	2B-1-AM	2B-2-AM	2B-3-AM
Wellhead pres.										
Mean (psia)	12.2099	11.6204	12.3896	11.7456	11.6094	12.7097	12.2991	12.1921	12.5166	12.3621
Standard Dev.	0.1170	0.1458	0.2195	0.1401	0.2165	0.0715	0.0919	0.2488	0.2034	0.0348
Min. (psia)	11.8402	11.2500	11.8877	11.5132	11.2081	12.5168	12.0423	11.4934	12.0150	12.2808
Max. (psia)	12.3762	12.1300	12.8220	12.0774	11.9474	12.9158	12.5234	12.5693	12.8196	12.4396
Gas prod. rate										
Mean (MMsfc/day)	0.2402	0.4774	0.6856	0.3858	0.3102	0.2707	0.1099	0.2255	0.4425	0.1545
Standard Dev.	0.0358	0.0385	0.0337	0.0159	0.0563	0.0122	0.0445	0.0920	0.0978	0.0274
Min. (MMsfc/day)	0.1606	0.4020	0.6207	0.3440	0.2379	0.2494	0.0367	0.0578	0.3046	0.1056
Max. (MMsfc/day)	0.3761	0.5710	0.7447	0.4196	0.4243	0.2934	0.1950	0.3933	0.6311	0.2042
Production duration (h)	4440	2976	3048	1032	456	1604	2263	3282	3601	703

change during dynamic subsidence. Thus, radial flow in the reservoir minimized the unknowns and simplified the flow occurring in this complex system. It was also assumed that the gob reservoir had no-flow upper and lower boundaries. This can be considered as a valid assumption since the slotted section of the venthole spanned almost all the methane emission sources and the entire length of the deformed section of overlying strata.

In the analyses, the production rate was used in multi-rate drawdown analyses. In gob gas venthole production, small changes in pressure result in changes in almost instant change in production rate without the need of waiting a long stabilization period. Therefore, it was assumed that, due to the high permeability of the gob environment, the gas production rate between consecutive rate changes and recorded measurements are constant allowing the analyses of the data using multi-rate drawdown techniques. In this environment pressure transients are short lived too.

Interference effects from other wells can affect the analyzed pressure data during well testing in producing fields. Ideally, a multiple well simulation model should be used for analysis using both proper rate history for each producer and accurate reservoir geometry. This way, the combined effects of neighboring wells can be added to the response of the tested well. However, considering that different wells may not produce from exactly the same layers or the well spacing and the geometry of the reservoir boundaries may be difficult to describe with an analytical model, this procedure becomes very cumbersome and frequently many approximations have to be made. In many cases, tests are analyzed with a single-well-model approach (Bourdet, 2003). Considering the complexity of the gob, a single-well-model approach was adopted in this study, too.

The models that are used in this study assume that the gob reservoir is homogeneous and is of single porosity despite the fact that there are various heterogeneities in the gob, including fractures, bedding plane separations, tension and compression zones. Even for conventional oil and gas reservoirs that do not experience major strata disturbances, there is not a single reservoir that is actually homogeneous. However, it has been suggested (Bourdet, 2003) that many reservoirs behave homogeneously during production and well test analyses. Therefore, in the absence of the information on the exact heterogeneities and their locations, the homogeneous model assumption is the most widely accepted one in well test analysis.

In this study, 2-zone composite radial models with vertical boreholes were used. The composite model assumes that the reservoir properties change at a certain radius from the borehole. This phenomenon does not necessarily occur in nature, although some reservoirs behave like they are composite. For instance, a borehole drilled in a naturally fractured reservoir with different fracture distributions around the well path may behave as composite reservoir. For a gob reservoir, this assumption can be considered as a valid one since the properties of gob change in the cross-panel direction due to subsidence and compaction. Thus, there may be a different flow capacity (kh) reservoir around the borehole to some distance into the gob in the radial direction, as compared to the rest of the gob reservoir.

The wellbore storage term was considered "zero" in the analyses presented in this paper. Usually, this term is needed when the compressibility of the wellbore fluid is not constant. Such situations may involve large drawdowns applied in gas wells or drastic changes in temperature in the borehole during production. In the study site, the GGVs were relatively shallow and, thus, there was not much of a temperature gradient. Also, the surface blowers were applying small suction pressures for gas production. Therefore, wellbore storage effects could safely be neglected under these circumstances.

The total, or apparent, skin factors calculated from the well tests were corrected for partial penetration effects. The ventholes monitored in this study were completed over the entire gob thickness (200 ft). However, they were communicating with the gob only through the slotted openings, which were approximately 2 in in width and 8 in in length, and were created approximately every 24 in in the casing (Fig. 2). The convergence of flow lines towards these slots might have created an additional pressure drop due to restricted flow entry as suggested by Brons and Marting (1961). Therefore, this pressure drop was dealt with as if it was a skin effect and labeled as the skin due to partial penetration or "pseudo-skin". This "pseudo-skin" effect was subtracted from the total skin to find the mechanical skin. Based on the frequency and dimensions of the slots, as well as the length of the completion interval, the b and h/r_w terms given in Brons and Marting (1961) and also in (Dake, 1978) were calculated as approximately as 0.33 and 5.8, respectively. Using these data in the graphs given in these references, the pseudo-skin factor was determined nearly as $+1$.

As it was mentioned earlier in this paper, the production rate-wellhead pressure histories of the ventholes were analyzed separately during panel mining (DM) and after panel completion periods (AM), since it is known that mining operation affects both reservoir-behavior and the gas in place for production from the gob. From the production and reservoir-behavior point of view, the DM stage can be considered when the reservoir is charged continuously with gas due to creation of new gob strata as the longwall face advances. Thus in this analysis, the DM period was considered as an infinite acting flow period before the occurrence of any boundary or transient-limiting effects.

In the AM phase, on the other hand, mining of the panel is stopped and the panel is completed (and sealed in some cases). These cases make the gas reservoir limited both in size and in gas in place and the gob may act as a bounded reservoir, in which case a pseudo-steady state acting period seems more appropriate to describe the flow during AM production. Pseudo-steady state (PSS) is a flow regime that occurs in bounded (closed) reservoirs after the pressure transient has reached all the boundaries of the reservoir. Thus, radial-composite models with no-flow outer boundary conditions were used with PSS flow conditions to analyze the AM production phase of the ventholes.

4.2. Brief theory of the well test analysis techniques used for the production data of this study

In multi-rate drawdown well test analysis, wells should ideally produce with a constant rate to reach stabilized flow conditions after a rate change, especially in low-permeability reservoirs. This is certainly a limitation in situations where it is difficult to control production rate. It is also a limitation for analyzing successive rate-pressure data points. In order for the analyses to be valid in such situations, the permeability of the reservoir should be high enough and the wellbore storage should be negligible so that the pressure transients will reach stabilization almost instantly after a rate change. In gob reservoirs, these conditions may be satisfied due to their very high permeabilities and the use of multi-rate testing theory in analyzing venthole production data may be justified.

4.2.1. Constant rate solution for radial flow-infinite acting period-of the venthole production (DM)

The constant rate solution for analyzing radial flow is (Fekete Associates, 2009):

$$\psi_i - \psi_{wf}(t) = 1.632 \times 10^6 \frac{q_g T}{kh}\left[\log\frac{kt_a}{\phi\mu_{gi}c_{ti}r_w^2} - 3.23 + 0.87s'\right] \quad (1)$$

where ψ is the real-gas pseudo-pressure that is used in place of pressure in natural gas engineering. It is defined as:

$$\psi(p) = 2\int_{p_b}^{p}\frac{pdp}{\mu Z} \quad (2)$$

Radial flow data will form a straight line when placed on a semi-log plot:

$$\psi_i - \psi_{wf}(t) = 1.632 \times 10^6 \frac{q_g T}{kh} \log(t_a) + 1.632 \times 10^6 \frac{q_g T}{kh} \left[\log \frac{k}{\phi \mu_{gi} c_{ti} r_w^2} - 3.23 + 0.87 s' \right] \quad (3)$$

The slope, m, of $\Delta\psi/q$ versus log t_a is used to calculate permeability by;

$$k = 1.632 \times 10^6 \frac{T}{mh} \quad (4)$$

Using Eq. (4) and the slope from $\Delta\psi/q$ versus log t_a plot, total skin (s') can be calculated using;

$$s' = 1.151 \left[\frac{\psi_i - \psi_{wf}}{m} - \log \frac{k t_a}{\phi \mu_{gi} c_{ti} r_w^2} + 3.23 \right] \quad (5)$$

The signature of radial flow on a derivative plot, on the other hand, is a horizontal straight line. The position of this line, along with the original data, may be used to calculate estimates of permeability and apparent total skin. The derivative, as defined $\frac{\Delta\psi}{\Delta \ln(t)}$, of radial gas flow equation is:

$$Der = 7.088 \times 10^5 \frac{q_g T}{kh} = \text{constant} \quad (6)$$

Thus,when the gas drawdown data is plotted log($\Delta\psi/q$) versus log (t_a), then the permeability and apparent skin can be determined from:

$$k = 7.088 \times 10^5 \frac{q_g T}{Der.h} \quad (7)$$

$$s' = 1.151 \left[\frac{\psi_i - \psi_{wf}}{2.303\, Der} - \log \frac{k t_a}{\phi \mu_{gi} c_{ti} r_w^2} + 3.23 \right] \quad (8)$$

The pseudo-skin due to partial penetration effects that was calculated as +1 for the ventholes in Section 4.1 should be subtracted from the total skin calculated using Eqs. (5) and (8) to find mechanical skin around ventholes.

4.2.2. Constant rate solution for pseudo-steady state phase—bounded reservoir—of the venthole production (AM)

The constant rate solution for analyzing pseudo-steady state is:

$$\psi_{wf} = \psi_i - 1.417 \times 10^6 \frac{q_g T}{kh} \left[\frac{0.000527 k t_a}{\phi \mu_{gi} c_{ti} r_e^2} + \ln\left(\frac{r_e}{r_w}\right) - \frac{3}{4} + s' \right] \quad (9)$$

This equation is linear with time and, thus, pseudo-steady state flow data forms a straight line when plotted on a Cartesian plot. In addition to determining k, r_e and s', the slope of $\frac{\Delta\psi}{q}$ versus time plot in PSS analysis can be used to find reservoir pore volume and gas in place using drawdown data:

$$V_p = \frac{2347 T}{m \mu_{gi} c_{ti}} \quad (10)$$

$$G = \frac{V_p (1 - S_{wi})}{B_{gi}} \quad (11)$$

The derivative analysis is carried out by taking the derivative of Eq. (9) with respect to the logarithm of time, which gives:

$$Der = \frac{2348 q_g T t_a}{A h \phi \mu_{gi} c_{ti}} \quad (12)$$

This result is linear with time and the derivative of PSS data on a log–log plot is a straight line with unit slope. Thus when log $\left(\frac{\Delta\psi}{q}\right)$ versus log (t_{PSS}) is plotted, it gives a straight line or a straight line trend in the plot.

Using well test analyses techniques briefly presented in this section, flow efficiency (FE) of a venthole can be calculated. FE is a relative index that is defined as the ratio of actual productivity index of a well to its productivity when there is no skin ($s' = 0$). Flow efficiencies of about 2.0 may be obtained after hydraulic fracturing in formations of moderately high permeability; in low permeability formations, the FE may reach 5.0 after a fracture treatment (Matthews and Russell, 1967). The relationship that was used in this study to calculate flow efficiency is:

$$FE = \frac{\overline{\psi}_R - \psi_{wf0}}{\overline{\psi}_R - \psi_{wf0} - 0.869\, m s'} \quad (13)$$

Similarly, the damage ratio (DR), which is also a relevant index, was calculated using:

$$DR = \frac{1}{FE} \quad (14)$$

Thus, higher FE and lower DR indicate better reservoir-flow properties and more productive boreholes.

4.2.3. Superposition in time

In order to apply the presented Eqs. (1)–(12) and techniques for multi-rate production histories, the "elapsed time" should be defined using the superposition theorem. This theorem mathematically states that any sum of individual solutions of a second order linear differential equation is also solution of the equation itself (Dake, 1978). Thus, superposition in time for a well producing with multiple rate conditions for various durations means that individual constant rate wells can be placed in the same position in the reservoir at any time and an expression for the resulting pressure distribution in time can be derived (Dake, 1978). The superposition time used in this study to analyze the data was:

$$t_n = \sum_{j=1}^{n} \frac{q_j - q_{j-1}}{q_n} \log(t - t_{j-1}) \quad (15)$$

$$\Delta t_n = \sum_{j=1}^{n} \frac{q_j}{q_n} \log \frac{t_n + \Delta t - t_{j-1}}{t_n + \Delta t - t_j} \quad (16)$$

4.3. Reservoir and fluid properties

Table 3 gives the reservoir and fluid data that was used in the F.A.S.T WellTest® software (2009) for calculating the test data and results. The data have been calculated based on full gas saturation ($S_g = 100\%$) in the gob and using average compositions of produced gas streams, average pressure and temperature conditions measured during the production periods and the published correlations (Reid et al., 1977). Porosity values of ~10% in DM between rock layers and for a newly formed gob determined from logs (Karacan, 2009), and 5% in AM due to compaction were used in the calculations.

Table 3
Reservoir and fluid data that have been used in the well test analysis.

	1B-1-DM	2B-1-DM	2B-2-DM	2B-3-DM	2B-4-DM	3B-1-DM	1B-1-AM	2B-1-AM	2B-2-AM	2B-3-AM
Well radius (ft)	0.29	0.33	0.33	0.29	0.29	0.29	0.29	0.33	0.33	0.29
c_f (1/psi)	1.68E−05	8.34E−05	1.09E−05	1.09E−05	1.09E−05	1.09E−05	1.09E−05	6.48E−05	1.75E−05	1.75E−05
c_t (1/psi)	1.32E−03	1.32E−03	1.32E−03	1.35E−03	1.33E−03	1.31E−03	1.31E−03	7.72E−03	1.33E−03	1.31E−03
c_g (1/psi)	8.34E−02	7.15E−02	7.17E−02	8.34E−02	8.34E−02	8.34E−02	8.34E−02	8.34E−02	8.34E−02	8.34E−02
Porosity (%)	10	10	10	10	10	10	5	5	5	5
$T_{wellhead}$ (F)	60	60	58.4	49.2	54.2	94	60	94.7	96.7	97.5
Z (comp. fact)	0.997	0.999	0.997	0.997	0.997	0.998	0.997	0.998	0.998	0.998
Gas Vis (cp)	0.0101	0.0103	0.0101	0.01	0.0102	0.0106	0.0101	0.0107	0.011	0.0108
B_g (bbl/scf)	0.1858	0.1862	0.1852	0.1959	0.1837	0.1981	0.1858	0.2136	0.1991	0.1993

5. Well test models and analysis results

Routine production tests are performed in the oil and gas industry for long-producing wells in order to identify productivity changes in the wells to manage the reservoir better. For instance, by measuring the flowing bottom-hole pressure with time for a constant production rate, it is possible to determine the parameters of permeability and skin by using the radial inflow equation. These tests are usually expensive and require sophisticated downhole instrumentation and analysis methods. However, the obtained data from these measurements and analyses are so helpful that they eventually are used as input to the reservoir simulation models for updating the reservoir parameters by history-matching the productions. Owing to the importance of the measurement techniques and the analyses methods, various researchers developed methods to test conventional oil and gas wells for a better understanding of reservoir parameters and improved reservoir management (Valvatne et al., 2003; Kuchuk and Onur, 2003; Escobar et al., 2007).

For unconventional wells, such as GGVs on the other hand, the development of specific testing and interpretation methods remained not existent. This was partly due to the difficulties associated with instrumentation of these ventholes because of safety concerns to the operating mine, partly due to the complexity of the gob reservoir created upon strata relaxation during panel mining, due to venthole stability issues, and partly due to the short production lives of the ventholes compared to conventional oil and gas wells. Despite these road blocks, the importance of understanding the properties of the gob reservoir is still of critical importance in order to control methane in the mining environment. This study presents a rare application of conventional gas well testing methods for analyzing GGV productions from gob reservoirs.

5.1. Data preparation and analysis methodology for GGV productions

The flow rate and pressure data should be as accurate as possible during the testing period. During data preparation, the flow data of the first several hours after venthole interception were eliminated from the production histories, since gas flow rates were changing rapidly and unreliably during initial installation and operation of the exhausters. Additionally, no special attempts, such as estimation, were made to introduce the missing rates in the production history when the rate data were missing due to exhauster malfunctions or instrumentation failures. These dates were treated as empty dates in the software. Also, no-flow rate simplification procedure was applied to the data set and the full and unfiltered production history was used as the multi-rate testing data.

Initially, test simulations were performed on linear scales using different interpretation models, defined on a single flow period as suggested by Bourdet (2003). This initial approach was adopted to check whether the interpretation models were applicable for the complete test sequence and to see if the selected model was applicable for long periods. This approach also enabled checking of the impact of the potential changes in venthole condition during production, which is not uncommon for GGVs due to dynamic subsidence.

Interpretation of well test data is an inverse problem for which more than one model can be found applicable to describe the pressure response. During the analysis of rate-pressure data obtained in this study, a representative interpretation model was first identified. Using diagnostic plots, radial flow in a homogeneous-composite reservoir during infinite acting (DM) and pseudo-steady-state acting (AM) flow periods were chosen as the interpretation models. These models were found to be more appropriate for the studied cases and for the measured data.

Fig. 7 schematically shows the two types of models chosen for the interpretation of gas venthole production data and the reservoir parameters.

The test simulations, using the models given in Fig. 7, were started with initial estimates of the reservoir and wellbore parameters, which were adjusted using F.A.S.T. WellTest's (Fekete Associates, 2009) APE (Automated Parameter Estimation) iteration algorithm to match the field data and to concurrently reduce the average error on three usual plots: log–log, semi-log superposition and linear scale test history. These plots focused on the complete flow and test sequence.

5.2. Results of tests and interpretation for GGVs and gob reservoirs

Figs. 8 and 9 show the example data matches for DM and AM phases of production, respectively, obtained for 2B-1 venthole using the models shown in Fig. 7. The calculated data and the model predictions for wellhead pressure histories on linear scale (C-plots), semi-log superposition (B-plots) and log–log scale (D-plots) are presented in the same plots for comparison purposes. In each figure, Plot-A is the measured gas rate and wellhead pressures used in the analyses. These figures show that the model predictions on linear, semi-log superposition and log–log data are generally good for both DM and AM production phases of 2B-1 venthole production. By using the data of these plots, average reservoir and wellbore skin parameters were calculated for 2B-1. Similar analyses were performed for each venthole. The results of these analyses for each venthole for their DM and AM production phases are given in Table 4.

Table 4 presents the findings of permeability and radius of investigation results in the first four rows of the tables for DM and AM flow periods of each venthole. For the DM flow period, the results show that the estimated permeabilities were highest, 1173 and 1544 md, around (Zone 1-Fig. 7) 2B-1 and 2B-2 ventholes, respectively. Permeability values around the other ventholes were calculated as 650–700 md. For 2B-1 and -2, the permeabilities calculated for the reservoir portion beyond the radius of Zone-1 were also highest. The permeability values calculated for Zone 2 for these ventholes were around 2000 md, as opposed to ~1000 md for the other ventholes except 2B-3, which had ~1500 md outside of Zone-1. However, it should be kept in mind that these average effective permeabilities were calculated for the whole 200 ft section open to flow through the casing slots using a homogeneous model. Thus, individual fractures or bedding plane separations might have higher permeabilities.

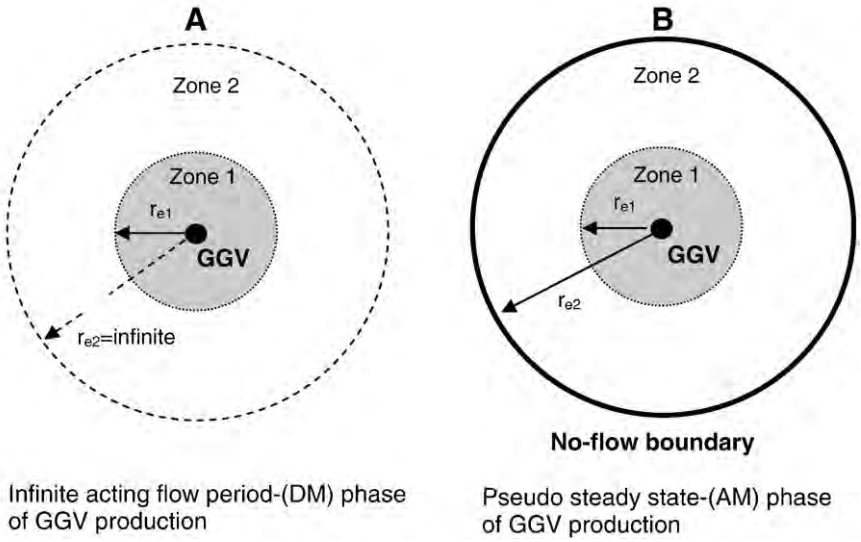

Fig. 7. Schematic representation of radial-composite models used in DM (A) and AM (B) phases of venthole production.

The radius of investigation of 3B-1 in Zone-1 was the largest of all ventholes with a calculated value of ~2820 ft. This venthole was followed with 2B-1 and 2B-2, whose radii of investigation values were ~1200 ft. On the other hand, 1B-1, 2B-3 and -4 had calculated Zone-1 radii values of 700–800 ft. However it should be emphasized that, although the radius of investigation is frequently viewed as the minimum radial distance to any event that will not be observed during the test period, the transient radius may be greater than the radius of investigation estimated from well tests due to layer permeability and saturation variations. This is certainly a valid observation for the current study due to the known existence of fractures and bedding layer separations during mining. Thus, due to the averaging effects of the interpretation results, the complete reservoir area affected by the well production may be confined in a different circular area around the wellbore (Oliver, 1990). The calculated radius of investigation from the well tests gives an approximate value and an order of magnitude idea about the true distance for the existence of boundaries (Matthews and Russell, 1967) rather than an exact distance.

In all of the ventholes, calculated total skins and the mechanical skins around the ventholes were high (increasing negative values)

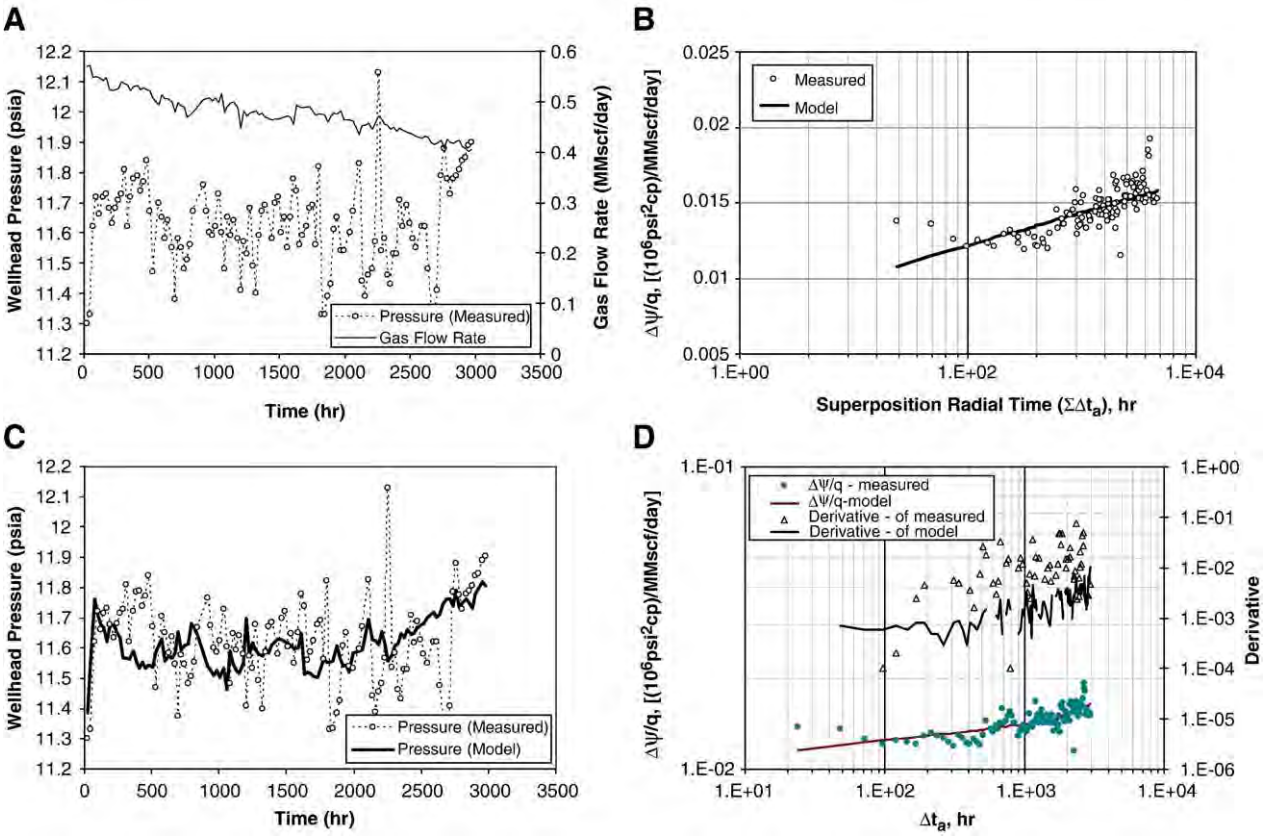

Fig. 8. Plots of gas flow rate-wellbore pressure (A), semi-log superposition time (B), linear pressure match (C) and log–log flow potential and derivative (D) for analysis of 2B-1 in DM period—radial infinite acting period.

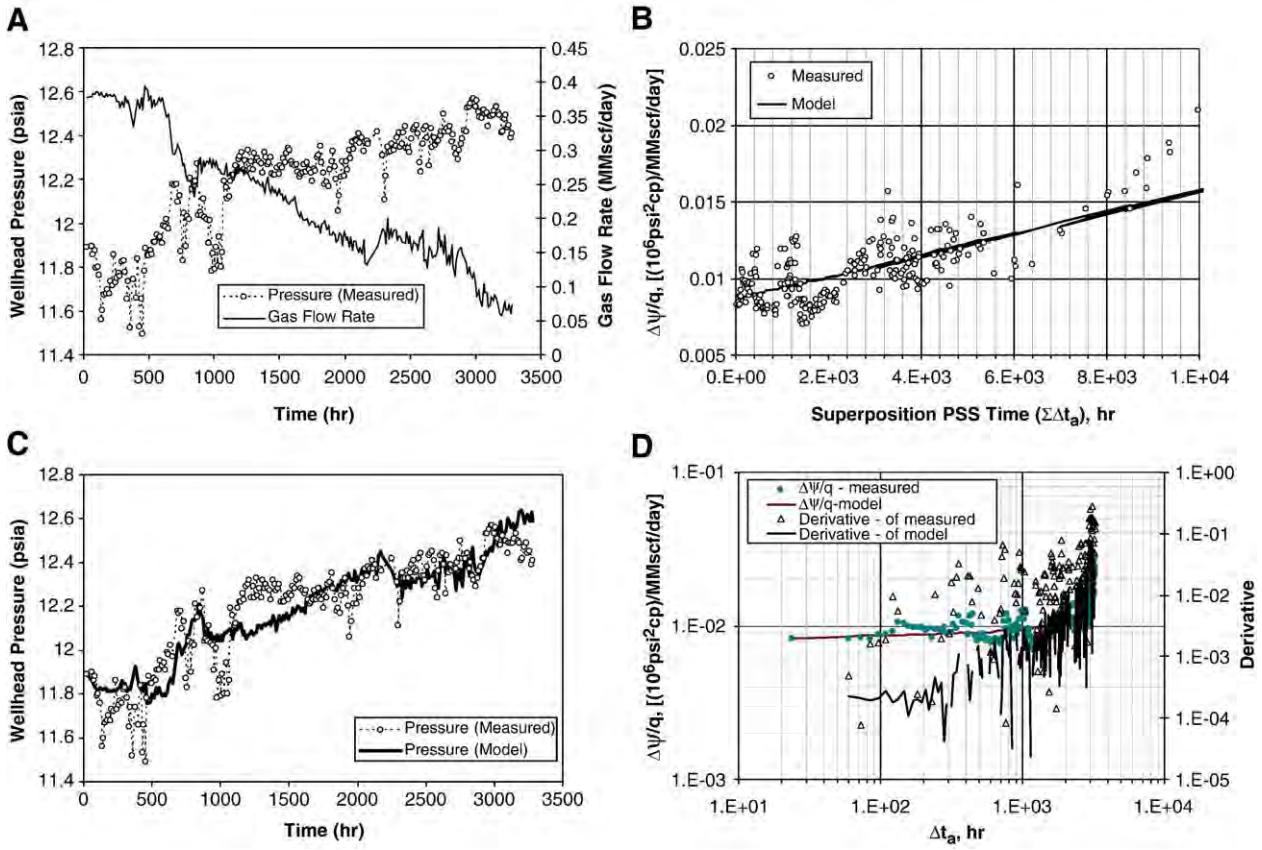

Fig. 9. Plots of gas flow rate-wellbore pressure (A), superposition time (B), linear pressure match (C) and log–log flow potential and derivative (D) for analysis of 2B-1 in AM period—radial pseudo-steady state acting period in closed reservoir.

meaning that the ventholes showed the properties of extensively fractured wells. These values were in agreement with the gob reservoir conditions generated during longwall mining as depicted in Fig. 1. The calculated skin values were also in agreement with the cumulative gas productions obtained from the ventholes and the flow efficiency values.

Table 5 shows methane and total gas productions and their average production rates, as well as methane percentages. These values can be compared with the calculated reservoir properties from the well tests. This table shows that 2B-2 had the highest cumulative gas and methane production, as well as highest production rates in DM flow phase. These data corroborates with 2B-2's permeability, radius of investigation and skin values shown in Table 4.

Table 4 also shows the average gob reservoir parameters calculated for the AM flow phase of gob gas ventholes using the model shown in Fig. 7-B. In using this model, it was assumed that the end of mining and sealing of the panel will create a bounded reservoir effect on the ventholes' productions in which the pressure transients reach the outer boundaries very quickly and start a pseudo-steady state flow period. Since the AM phase of flow was monitored for only four of the ventholes, the analyses were performed using that data.

For the AM phases of productions, the calculated permeabilities were highest in Zone-1 of 1B-1 and 2B-1 with values of 864 md and 1937 md, respectively. Radii of these zones extended approximately to 1790 ft and 580 ft from 1B-1 and 2B-1, respectively. However, the total and mechanical skins were lower in these ventholes compared to other two ventholes (2B-2 and 2B-3) that had somewhat lower permeabilities within a smaller near-venthole zone, particularly for 2B-2. The outer zones of the gob reservoirs around these ventholes were generally large (6000–9000 ft), except 1B-1, and had high

Table 4
Results of multi-rate well tests analyses for DM and AM flow periods of all monitored gob gas ventholes.

	1B-1-DM	2B-1-DM	2B-2-DM	2B-3-DM	2B-4-DM	3B-1-DM	1B-1-AM	2B-1-AM	2B-2-AM	2B-3-AM
r_{e1} (ft)	729.2	1198.9	1218.9	781.7	781.6	2818.2	1787.3	579.8	360.8	620.5
k_{re1} (md)	651.9	1173.0	1543.8	700.2	715.6	633.6	864.7	1937.1	524.1	405.0
r_{e2} (ft)	inf.	inf.	inf.	inf.	inf.	inf.	2062.3	9179.2	9173.8	6300.1
k_{re2} (md)	1050.0	1974.4	2145.8	1581.2	899.0	1076.8	1466.6	10788.2	15648.5	11223.5
Total skin (s′)	−6.2	−5.5	−7.9	−7.4	−5.2	−8.4	−2.4	−3.6	−6.1	−5.5
Mech. skin	−5.2	−4.5	−6.9	−6.4	−4.2	−7.4	−1.4	−2.6	−5.1	−4.5
Final rate (MMscf/day)	0.161	0.406	0.671	0.379	0.264	0.256	0.049	0.073	0.317	0.189
Cum. prod. (MMscf)	44.489	59.143	87.328	16.606	5.776	28.124	10.933	31.046	68.803	4.580
Final flow pressure (psia)	12.3	11.9	12.1	11.6	11.9	12.7	12.2	12.4	12.6	12.4
Ave. error (%)	0.98	1.08	0.88	0.77	1.14	0.47	1.83	0.79	0.70	0.86
FE	2.3	2.2	3.9	5.6	2.1	5.4	1.4	1.8	8.2	3.2
DR	0.4	0.5	0.3	0.2	0.5	0.2	0.7	0.5	0.1	0.3

Table 5
Cumulative gas and methane productions, and their production rates from each ventholes in DM and AM phases of flow.

Venthole/ flow phase	Average CH_4 (%)	Average gas (CH_4 + Air) rate (MMscf/day)	Cumulative gas production (MMscf)	Average CH_4 rate (MMscf/day)	Cumulative CH_4 production (MMscf)
1B-1-DM	90.5	0.240	44.48	0.220	40.77
2B-1-DM	40.2	0.477	59.14	0.192	23.75
2B-2-DM	46.2	0.685	87.32	0.317	40.23
2B-3-DM	53.8	0.385	16.60	0.209	8.98
2B-4-DM	45.7	0.310	5.77	0.139	2.64
3B-1-DM	87.5	0.270	28.12	0.238	15.90
1B-1-AM	75.7	0.109	10.93	0.086	8.13
2B-1-AM	40.8	0.225	31.04	0.088	12.10
2B-2-AM	59.2	0.442	68.80	0.252	37.83
2B-3-AM	39.8	0.154	4.58	0.061	1.79

permeabilities (11,000–16,000 md). The highest permeability (~15,650 md) and one of the largest influence zones (~9174 ft) was calculated for 2B-2. This borehole had the highest skin (−6) and the highest flow efficiency (8.2), which resulted in the highest methane and cumulative gas production and the highest production rates (Table 5). Although 2B-3 had also a high skin value, reasonably high permeabilities and large influence zones, its production rate and cumulative production were low.

Although the reservoir and borehole data calculated using well testing methods generally corroborates the productivity of the ventholes, the well test results are average values based on the homogeneity assumption of the well test model. Therefore, the properties of individual heterogeneities may not be well represented in this approach. Furthermore, there are other factors that affect properties of gob reservoirs and the productivity of gob gas ventholes, such as tension and compression zones and the location of the ventholes with respect to these zones. It has been established in the introduction section that the caving action and formation of a gob reservoir are very complex and highly dependent on the strata. In such an environment, the location of the ventholes is of critical importance. The ventholes, when they are located close to the entries and particularly tailgate entries (Fig. 4), produce better since they stay in the tension zone compared to the center locations, which are under compression. 2B-2 is one of those ventholes that was located closest to the tailgate entry of the second panel.

Specific to this site, there was a sandstone channel with varying thicknesses above the mined coal bed, which spatially replaced the weak shale units (Fig. 4). 2B-2 and 3B-1 were located where there was no sandstone above the coal bed. 1B-1 and 2B-1 were drilled where the sandstone thickness was between 0 and 20 ft, and 2B-3 and 2B-4 were located where sandstone thicknesses were >20 ft and 40 ft, respectively (Fig. 4). The presence of this sandstone and its thickness below the ventholes affected both caving behind the shields and the fracturing of the overlying strata. Interpretation of well test results (Tables 4 and 5) along with the sandstone channel thickness below the ventholes generally suggest that when it is absent or thin, the well test calculated permeability of gob reservoir around the ventholes and radii of investigations are larger. In these boreholes, high negative skins and high flow efficiencies are also observed. These calculations corroborate the total gas and methane production potentials (Table 5) of the ventholes drilled in locations where sandstone was thin or washed out, as opposed to ventholes drilled in thick portions of this sandstone (2B-3 and 2B-4).

This study and the approach undertaken suggest that conventional well test techniques can be a promising way to evaluate complex gob reservoirs and to assess gob gas venthole performance for safety purposes during longwall mining and for optimizing methane capture. However, the well test results should be interpreted with the integration of local geological and geophysical data, as commonly practiced in oil and gas industry.

6. Summary and conclusions

The ability to analyze the gob gas venthole data and to reconcile gob properties is important for designing better methane control strategies to improve the safety of the underground workforce and to improve methane capture from the gob as a clean fuel. This study presented an effort for application of well test analysis techniques for determination of gob reservoir properties and gob gas venthole performances.

Wellhead gas production rates and pressures were monitored for 6 ventholes located on adjacent panels during and after mining. Since these two stages potentially resulted in varying gob reservoir characteristics and gas capacities, they were analyzed separately using two different models. Multi-rate well test techniques were used for both situations. The application of these techniques was justified given the high permeability of the gob reservoir which enabled almost instant stabilization of pressure after a rate change at the wellhead.

The results showed that conventional well test analyses methods can be used for the appraisal of gob characteristics, such as permeability around the venthole and out in the gob, radius of investigation, total and mechanical skin around the ventholes and the ventholes' flow efficiencies and damage ratios.

The results specific to this study and the mine site showed that although the gob reservoir and venthole data calculated using well testing methods generally corroborated the productivity of the ventholes, there were other factors that should be considered in evaluations. For instance, reservoir heterogeneities during caving and formation of the gob were very complex and were highly dependent on the local strata. In such an environment, the locations of the ventholes were of critical importance. This study proved that ventholes located close to the entries, particularly tailgate entries, produced better.

The presence of the sandstone channel and its thickness below the ventholes affected both caving behind the shields and the fracturing of the overlying strata. Interpretation of well test results along with the sandstone channel thickness below the ventholes generally suggested that when the sandstone was absent or thin, the well test calculated permeability of the gob reservoir around the ventholes and the radius of investigations predicted in the gob were larger. In these boreholes, high negative skins and high flow efficiencies were also observed. Quantitative well test results corroborated with the total gas and methane production potentials of these ventholes and their locations with respect to the spatial thickness of the sandstone.

It was shown that conventional well test techniques could be a valuable tool for reconciling gob gas reservoirs and gob venthole performances since there is no other more effective alternative. Owing to the complexity of the system, model choice should be performed with care and by considering the details due to mining effects. Furthermore, local geology and geophysical data, as well as proven caving characteristics, should be integrated into the

interpretation of well test results and into the methane control-system design process.

Nomenclature

A	drainage area	m^2	ft^2
B_g	formation volume factor	–	–
c	compressibility	kpa^{-1}	psi^{-1}
DR	damage ratio	–	–
FE	flow efficiency	–	–
h	net pay	m	ft
k	permeability	md	md
kh	flow capacity	md.m	md.ft
k/μ	mobility	–	–
kh/μ	transmissivity	–	–
m	slope of transient plots	–	–
P	pressure	kPa	psia
P_i	initial pressure	kPa	psia
P_R	average reservoir pressure	kPa	psia
P_{tf}	flowing wellhead pressure	kPa	psia
P_{wf}	flowing sandface pressure	kPa	psia
q_j	jth flow rate	m^3/d	scf/d
q_n	nth flow rate	m^3/d	scf/d
r_e	external radius, or radius of investigation	m	ft
r_w	wellbore radius	m	ft
s	skin factor	–	–
s'	apparent skin factor	–	–
S_g	saturation (gas)	–	–
t	time	h	h
t_a	pseudo-time	h	h
t_n	nth flow period, or superposition time	–	–
Ψ	pseudo-pressure for gas	$kPa^2/Pa.s$	$psia^2/cp$

Subscripts

f	formation or flowing
g	gas
i	initial
w	wellbore

References

Bourdet, D., 2003. Practical aspects of well-test interpretation. In: Cubitt, J. (Ed.), Handbook of Petroleum Exploration and Production. Elsevier, Amsterdam, pp. 351–375.

Brons, F., Marting, V.E., 1961. The effect of restricted fluid entry on well productivity. Journal of Petroleum Technology 172–174 February.

Cui, X., Wang, J., Liu, Y., 2001. Prediction of progressive surface subsidence above longwall coal mining using a time function. International Journal of Rock Mechanics and Mining Sciences 38, 1057–1063.

Dake, L.P., 1978. Fundamentals of Reservoir Engineering. Elsevier, Amsterdam. 443 pp.

Diamond, W.P., 1994. Methane control for underground mines. U.S. Department of Interior, Bureau of Mines Information Circular No: 9395. 44 pp.

Earlougher, R.C., 1977. Advances in Well Testing. Society of Petroleum Engineers of AIME, Dallas, TX. 264 pp.

Engler, T., Tiab, D., 1996. Analysis of pressure and pressure derivative without type curve matching, 4. Naturally fractured reservoirs. Journal of Petroleum Science and Engineering 15, 127–138.

Escobar, F.H., Ibagon, O.E., Montealegre, M., 2007. Average reservoir pressure determination for homogeneous and naturally fractured formations from multi-rate testing with the TDS technique. Journal of Petroleum Science and Engineering 99, 204–212.

Fekete Associates (2009). F.A.S.T. WellTest v. 7.1.1. http://www.fekete.com/software/welltest/description.asp.

Gale, W., 2005. Application of computer modeling in the understanding of caving and induced hydraulic conductivity about longwall panels. proceedings of Coal2005, 6th Australasian Coal Operator's Conference, Brisbane, Australia, pp. 11–15.

Karacan, C.Ö., 2009. Reservoir rock properties of coal measure strata of the Lower Monongahela Group, Greene County (Southwestern Pennsylvania), from methane control and production perspectives. International Journal of Coal Geology 78, 47–64.

Karacan, C.Ö., Goodman, G.V.R., 2009. Hydraulic conductivity and influencing factors in longwall overburden determined by using slug tests in gob gas ventholes. International Journal of Rock Mechanics and Mining Sciences 46, 1162–1174.

Karacan, C.Ö., Diamond, W.P., Esterhuizen, G.S., Schatzel, S.J., 2005. Numerical analysis of the impact of longwall panel width on methane emissions and performance of gob gas ventholes. Proceedings 2005 International Coalbed Methane Symposium, Paper No. 0505, Tuscaloosa, Alabama.

Karacan, C.Ö., Esterhuizen, G.S., Schatzel, S.J., Diamond, W.P., 2007. Reservoir simulation-based modeling for characterizing longwall methane emissions and gob gas venthole production. International Journal of Coal Geology 71, 225–245.

King, G.R., Ertekin, T., Schwerer, F.C., 1986. Numerical simulation of the transient behavior of coal-seam degasification wells. SPE Formation Evaluation 165–183 April.

Kuchuk, F.J., Onur, M., 2003. Estimating permeability distribution from 3D interval pressure transient tests. Journal of Petroleum Science and Engineering 39, 5–27.

Lee, J., 1982. Well Testing. Society of Petroleum Engineers of AIME, Dallas, TX. 159 pp.

Li, S., Lin, H., Cheng, L., Wang, X., 2005. Studies on distribution pattern of and methane migration mechanism in the mining-induced fracture zones in overburden strata. Proceedings of 24th International Conference on Ground Control in Mining, Morgantown, WV, pp. 268–273.

Liu, J., Elsworth, D., 1997. Three-dimensional effects of hydraulic conductivity enhancement and desaturation around mine panels. International Journal of Rock Mechanics and Mining Sciences 34, 1139–1152.

Lunarzewski, W.L., 1998. Gas emission prediction and recovery in underground coal mines. International Journal of Coal Geology 35, 117–145.

Luo, Y., 1989. An integrated computer model for predicting surface subsidence due to underground coal mining (CISPM). PhD dissertation, Department of Mining Engineering, West Virginia University, Morgantown, WV.

Markowski, A., 1998. Coalbed methane resource potential and current prospect in Pennsylvania. International Journal of Coal Geology 38, 137–159.

Matthews, C.S., Russell, D.G., 1967. Pressure Buildup and Flow Tests in Wells. Society of Petroleum Engineers of AIME, Dallas, TX. 172pp.

Mavor, M.J., Saulsberry, J.L., 1996. Testing coalbed methane wells. In: Saulsberry, J.L., Schafer, P.S., Schraufnagel, R.A. (Eds.), A Guide to Coalbed Methane Reservoir Engineering. Gas Research Institute, Chicago, IL. Chapter 5.

Mohaghegh, S., Ertekin, T., 1991. A type-curve solution for coal seam degasification wells producing under two-phase flow conditions. Proceedings of 66th Annual Technical Conference and Exhibition of Society of Petroleum Engineers, Dallas, TX.

Nashawi, I.S., 2008. Pressure transient analysis of infinite-conductivity fractured wells producing at high flow rates. Journal of Petroleum Science and Engineering 63, 73–83.

Oliver, D.S., 1990. The averaging process in permeability estimation from well-test data. SPE Formation Evaluation 319–324 Sept.

Palchik, V., 2002. Use of Gaussian distribution for estimation of gob gas drainage well productivity. Mathematical Geology 34, 743–765.

Palchik, V., 2005. Locatization of mining-induced horizontal fractures along rock layer interfaces in overburden: field measurements and prediction. Environmental Geology 48, 68–80.

Pappas, D.M., Mark, C., 1993. Behavior of simulated longwall gob material. Report of Investigations No. 9458, US Dept. of Interior, US Bureau of Mines. 39 pp.

Penn State University Libraries, 2000. Description of the geology of Greene County Pennsylvania. URL: http://www.libraries.psu.edu/emsl/guides/X/greene.htm.

Reid, R.C., Prausnitz, J.M., Sherwood, T.K., 1977. The Properties of Gases and Liquids. McGraw-Hill, New York, NY. 688 pp.

Ren, T.X., Edwards, J.S., 2002. Goaf gas modeling techniques to maximize methane capture from surface gob wells. In: Euler De, Sauza (Ed.), Mine Ventilation, pp. 279–286.

Singh, M.M., Kendorski, F.S., 1981. Strata disturbance prediction for mining beneath surface waters and waste impoundments. Proceedings of 1st International Conference on Ground Control in Mining, Morgantown, WV, pp. 76–89.

Thakur, P.C., 2006. Coal seam degasification. In: Kissell, F. (Ed.), Handbook for Methane Control in Mining: National Institute for Occupational Safety and Health Information Circular No: 9486, Pittsburgh, PA, pp. 77–96.

Tomita, S., Deguchi, G., Matsuyama, S., Li, H., Kawahara, H., 2003. Development of a simulation program to predict gas emission based on 3D stress analysis. Proceedings of 30th International Conference of Safety in Mines Research Institutes, South African Institute of Mining and Metallurgy, pp. 69–76.

Valvatne, P.H., Serve, J., Durlofsky, L.J., Aziz, K., 2003. Efficient modeling of nonconventional wells with downhole inflow control devices. Journal of Petroleum Science and Engineering 39, 99–116.

Whittles, D.N., Lowndes, I.S., Kingman, S.W., Yates, C., Jobling, S., 2006. Influence of geotechnical factors on gas flow experienced in a UK longwall coal mine panel. International Journal of Rock Mechanics and Mining Sciences 43, 369–387.

Whittles, D.N., Lowndes, I.S., Kingman, S.W., Yates, C., Jobling, S., 2007. The stability of methane capture boreholes around a longwall coal panel. International Journal of Coal Geology 71, 313–328.